J Fail. Anal. and Preven.
https://doi.org/10.1007/s11668-023-01815-4

CASE HISTORY—PEER-REVIEWED

# Failure Analysis of Glass Fibre Reinforced Plastic Pipe Produced by Filament Winding Technique

**Souvik Das · Gulshan Kumar · Ravikrishna Chatti · Soumendu Monia · Sunita Dey · Anup Kumar · Goutam Mukhopadhyay**

Submitted: 3 September 2023 / in revised form: 20 October 2023 / Accepted: 29 October 2023


**Abstract** The filament winding technique is the second popular process in basic composite manufacturing processes, which can provide an automated technique compared to traditional hand layup process. The continuous filament winding process is the manufacturing of glass reinforced polymer (GRP) pipes from continuously flowing glass fibre by winding it on an automatic machine. It is quick and reliable technology for making high performance parts. A big advantage of filament winding is that it uses continuous fibres which leads to very good material properties for both strength and stiffness. However, if there is any process abnormality it can cause defects such as voids, delamination, wrinkles, etc. which causes production loss or failure at customer loss leads to monetary and reputation loss. There was premature failure of GFRP composite pipes during hydrostatic (hydro) testing while laying out in the site were received. Two pipe samples, one referred as new or good pipe and another referred as leaked during hydro test, were investigated to find out the root cause of failure. The investigation consisted of field visits, studying the layout procedure, visual observation, microstructural characterization, thermogravimetric analysis (TGA) Fourier transform infrared spectroscopy (FTIR) and Raman analyses. Visual observations of the hydro test failed sample reveal some abnormal features like delamination of layers, circumferential cracks and white spots, while the leaked or used pipe shows features like air pockets, adherent foreign/ earthy materials, visible fibres and heterogeneity in colours. Adherence of earthy material on pipe's surface indicates that there is incomplete curing of polymer. Microstructural analysis exhibits that the volume fraction of fibres was very less (particularly in used pipe) in resin matrix and their distribution was also uneven. Raman, FTIR and TGA analysis suggest that impure or mixed resin material is used for production of pipe which failed during hydro test. Overall analysis suggests a defective manufacturing process and usage of expired polymer and sand along with non-prescribed fibre loading which might have initiated the failure of pipes during hydro test.

**Keywords** Glass fibre reinforced plastic pipe · Filament winding technique · Derivative thermogravimetric · Hydrostatic (hydro) testing · Resin

## Introduction

There are numerous composite fabrication processes to produce composite products, which are summarized (Fig. 1a) distribution of composite market in Indian. The filament winding technique is the second popular process in basic composite manufacturing processes, which can provide an automated technique compared to traditional hand layup process. The cost of composite production is an essential factor to restrict process development. It is concluded that filament winding process is used a relatively lower equipment cost, which can have a potential composite market in filament winding technique.

The process is commonly designed to pass the fibre through a resin bath and impregnated fibre can be wound on the mandrel with tension device [1]. Different fibre

S. Das (✉) · G. Kumar · R. Chatti · S. Monia · S. Dey · A. Kumar · G. Mukhopadhyay
Department of Scientific Services, Metallography Laboratories, Tata Steel Limited, Jamshedpur, India
e-mail: souvik.das@tatasteel.com

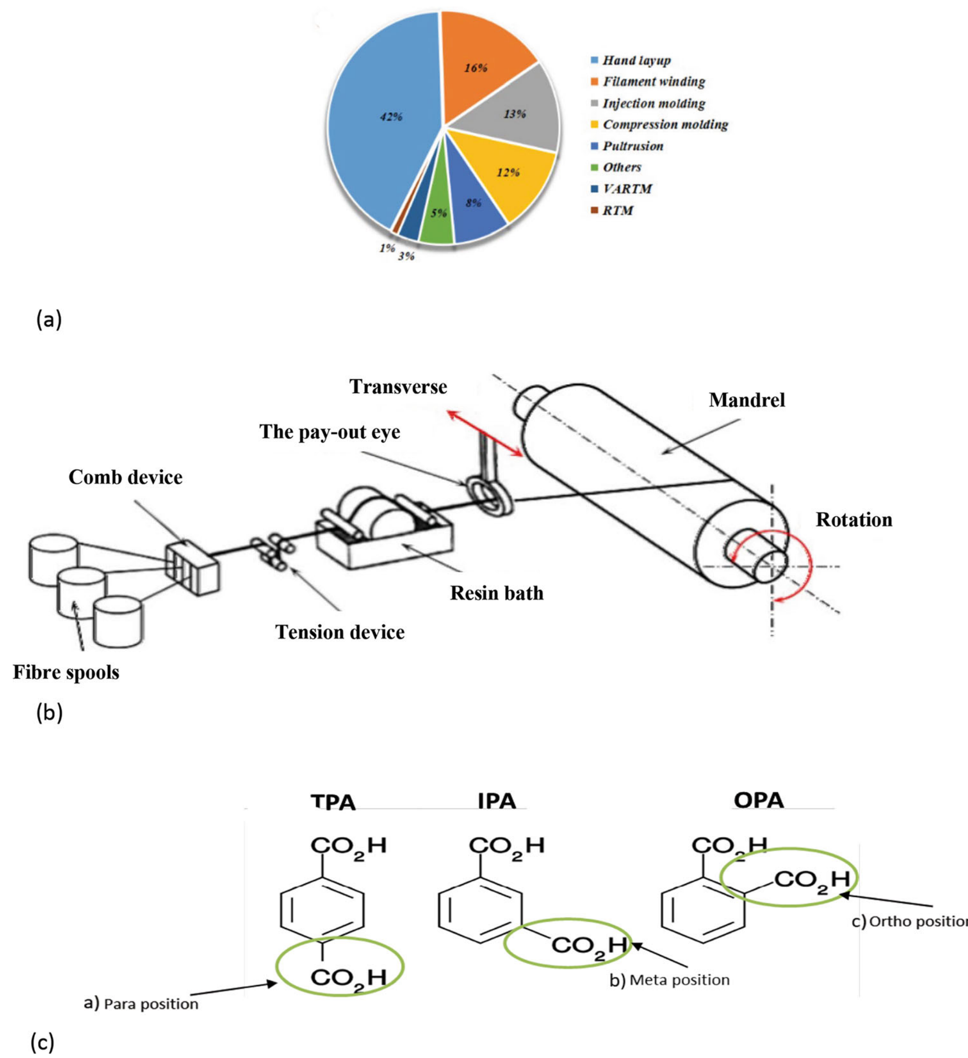


**Fig. 1** Composite fabrication processes: (**a**) distribution of composite market in Indian (**b**) Schematic diagram of filament winding technique (**c**) Isomers of phthalic acid: (**a**) TPA; (**b**) IPA and (**c**) OPA

spools are placed on creel device and mounted on the horizontal carriage. It can be controlled using different relative speeds to ensure filament winding angle or fibre orientation (Fig. 1b).

Filament wound composite product can be removed from the mandrel after the curing process accordingly, which may use hydraulic rams to remove completely. Curing of the laminate develops depending on the heat. Direct heating of the laminate is ensured by heating elements. Laminate temperature is measured on the cure region from various points. Temperature distribution is monitored on the PC monitor graphically. In some cases, the mandrel can become an integral part of the assembling product. By the motion of the mandrel under the control of the programmable logic controller (PLC) and the computers (PC), the glass fibre, the resin, the filling material and the surface materials are applied by precision measurements. Filament winding technique can provide a higher fibre volume fraction compared to other composite fabrication processes, which is one of strengthens in this processing technique. The continuous filament winding process is the manufacturing of glass reinforced polymer (GRP) pipes from continuously flowing glass fibre by winding it on an automatic machine. The inner and outer walls of the pipe are constructed by pressing glass fibre and resin together, and filling material (sand) is then added [2, 3] based on ASTM standards for GRP pipes [4–6]. As a result of reinforcing a high ratio of polyester by glass fibre, the inner and outer surfaces of the pipe become extremely robust against chemicals. Since the mid-section of the pipe is highly durable, the required stiffness is obtained, and the resistance against working pressures is obtained throughout the length of the pipe. Standard GRP pipes are manufactured using orthophthalic or terephthalic unsaturated polyester resin. The orthophthalic resin is the cheapest and the most used but with the most limited properties. In the case of special design requirements to meet specific properties, manufacture generally use isophthalic and vinyl


**Fig. 2** (**a**, **b**) Site visit images at one of the locations (Graveyard) (**c**) Leakage through main pipe body (**d**) Coupler joint lamination where seepage was observed (**e–i**) Visual observations of unused pipe sample reveals abnormal features

ester resin. Isophthalic resin demonstrates good acid resistance, moderate solvent resistance, good temperature resistance and high strength. It is corrosion, temperature, solvent and fuel resistant with superior mechanical properties. Purity of the resin material can be related to the identification of peak assignments for the starting materials of the resin such as phthalic acid and ethylene glycol (EG) and the polymerized product, polyethylene terephthalate (PET), respectively (Fig. 1c). Here, it is noteworthy, that phthalic acid can exist in 3 isomeric forms such as

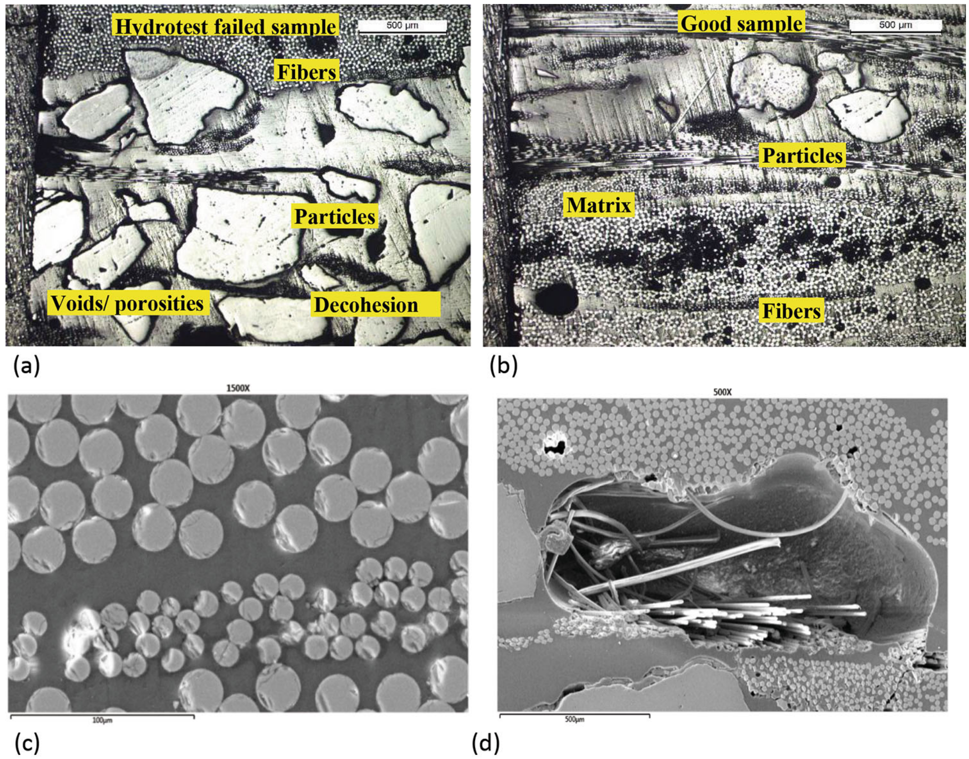


**Fig. 3** (**a**) Microstructural examination of hydro failed pipe (**b**) Microstructural examination of good pipe (**c**) Non-uniform and varying size of fibres of hydro failed pipe (**d**) Large void with entangled fibres trapped inside hydro failed pipe

terephthalic acid (TPA), isophthalic acid (IPA) and orthophthalic acid (OPA) based on the position of the carboxyl groups [7, 8] on the benzene ring. During manufacturing process, the PLC-PC modules provide an integrated process control in line with the pre-programmed designs. Basic data, such as diameter, stiffness and pressure class are entered into the programme. The PC calculates all the setting values of the machine. The process parameters and the thickness of the pipe are continuously monitored, and traceability is provided by storing these data. A cutting unit compatible with the pipe, which has an axial and radial stroke, enables the pipe to be cut smoothly and perpendicularly. Cutting operations take place automatically by entering the length of the pipe into the control system. Pipes that have been cut are transferred to specifically designed lifting stands, then to the chamfering and calibration section and from there to hydrostatic test section. In this present work, failure analysis of GRP pipe during hydrostatic test was carried out to find the geneses of failure and improve its service life.

## Experimental Procedure and Results

### Site Visit

Site visit was done in graveyard area where a 270-m length GFRP pipeline was laid (Fig. 2a and b). The then condition of site was not consistent to that of required for installation.

**Table 1** EDX analysis (wt.%) of particles in the matrix for hydro test failed sample

| Spectrum label | 1 | 2 | 3 | 4 | 5 | 6 |
|---|---|---|---|---|---|---|
| C | 5.19 | 7.63 | | 4.87 | 40.86 | 75.32 |
| O | 50.43 | 49.62 | 50.79 | 50.28 | 33.27 | 24.68 |
| Al | | | | | 3.56 | |
| Si | 44.38 | 42.75 | 49.21 | 44.85 | 13.87 | |
| Ca | | | | | 8.43 | |
| Total | 100.00 | 100.00 | 100.00 | 100.00 | 100.00 | 100.00 |

However, as per the construction team member present there, there was no maintenance of site for the previous few months. So, no conclusive remarks can be made about soil conditions. Hydrostatic test was carried out to find the internal soundness of the pipe before final laying. The test involves filling the vessel or pipe system with water, which stained to aid in visual leak detection, and pressurization of the vessel to the specified test pressure as per ASME B31 [9]. Pressure tightness was tested by shutting off the supply valve and observing whether there is a pressure loss. During laying of pipe of around 4500 m long leakage was observed during hydrostatic test. Hydrotest were carried out in all 9-10 locations, where pipeline was laid. At all locations, leakage along the joints was observed (Fig. 2c), lamination was done at all the joints where leakage was

**Table 2** Raman spectroscopy analysis

| Hydrotest failed Pipe | Peak assigned to | PET | TPA | TPA | TPA | TPA | EG |
|---|---|---|---|---|---|---|---|
| | Peak Position ($cm^{-1}$) | 1723 | 850 | 220 | 1324 | 1606 | 997 |
| | Solid | √ | √ | √ | √ | √ | √ |
| Good Pipe | Peak assigned to | IPA | OPA | OPA | OPA | EG | |
| | Peak Position ($cm^{-1}$) | 853 | 1491 | 785 | 1582 | 999 | |
| | Solid | √ | √ | √ | √ | √ | |

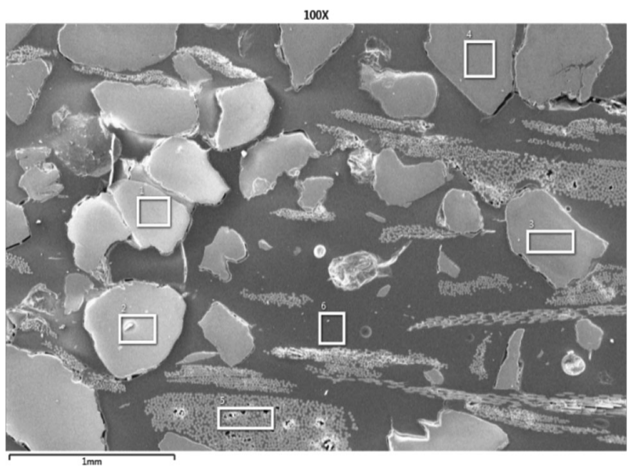


**Fig. 4** EDX analysis of the hydrotest failed pipe sample

observed (Fig. 2d). After providing lamination at joints, leakage was stopped however hydrotest failed as pressure droppage was observed due to seepage from the main pipe body and leakage could not be detected since most part of pipeline is underground and not visible, except joints.

### Visual Observation

Two sets of GRP pipe samples were collected from the manufacturer and construction site for characterization to find out the root cause of failure. The hydrotest failed pipe where leakage was found during testing was collected from the construction site. However, the leaked sample has a coupler joint within it and a thick layer of lamination was observed on it. Therefore, the location of leakage is not clear. Good pipe refers to the part of pipe which was passed though hydro test. Visual observations of leaked pipe sample reveal some abnormal features like reveals 2 abnormal features like delamination of layers, crack marks, circumferential cracks, and white spots (Fig. 2e, f, g, h, and i). Circumferential cracks are caused due to excess resin cured without glass fibre reinforcement, or resin cured at too high a temperature. Delamination of layers are caused due to too much sand being added during the manufacturing process. In certain locations air pockets, adherent foreign materials, visible fibres, and heterogeneity of colours were also observed. Visual observations of good pipe sample don't reveal any such abnormal features.

### Pipe Stiffness (PS)

Pipe stiffness is a characteristic to consider when selecting a flexible pipe used to underground. The pipe needs to have enough stiffness to withstand the handling and construction loads that it will be subjected to during installation. In poorer grades of backfill, it can have some impact on the long-term deflections of the installation. Thus, pipe stiffness is one of the important features for the quality inspection of GRP pipes.

Pipe internal diameter (*ID*) = 500 mm

Mean pipe radius = 254.2 mm

Liner thickness (*Tl*) = 1 mm

Structural wall thickness (*t*) = 6.4 mm

Total wall thickness (*Tt*) = Tl + t = 7.4 mm

Moment of inertia of unit length $(I) = Tt^3/12 = 33.7686667\ mm^4/mm$

Pipe stiffness $(PS) = ExIx10^6/0.149\ (r + \Delta y_t/2)^3$

Ring flexural modulus (*E*) = 21.5 GPa

Vertical pipe deflection $(\Delta y_t) = 25$ mm

Minimum pipe stiffness $(F/\Delta y) = 248$ kPa (As per ASTM D2412, where *F* is the recorded load on pipe [10])

Pipe stiffness (*PS*) = 256.860343 kPa

So, $PS \geq ((F/\Delta y)$, thus the pipe stiffness in more than minimum pipe stiffness safety factor.

### Microstructural Analysis

The samples were prepared in Baincut HSS Precision cutoff machine at low-speed diamond saw for the precision cutting of a GRP pipe micro sample. Samples were cut with minimal damage and deformation. Variable wheel rotation speeds were used range from 100 to 200 rpm for cutting the GRP pipes. The microstructure of the GRP pipe was analysed by optical microscopy and field emission gun scanning electron microscope (FEG-SEM) to observe the qualities of the different materials and the distribution of

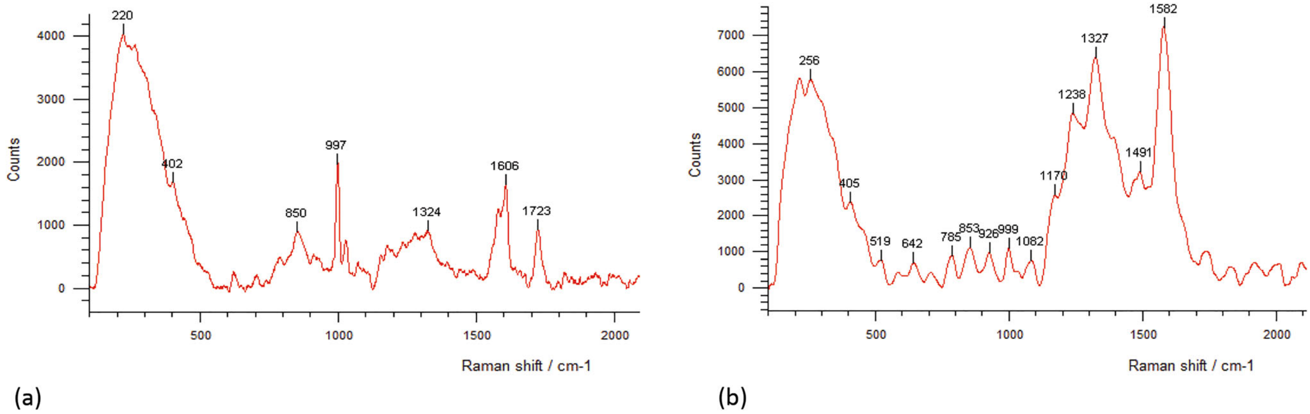


**Fig. 5** Raman spectroscopy analysis (**a**) hydrotest failed pipe sample (**b**) good pipe sample

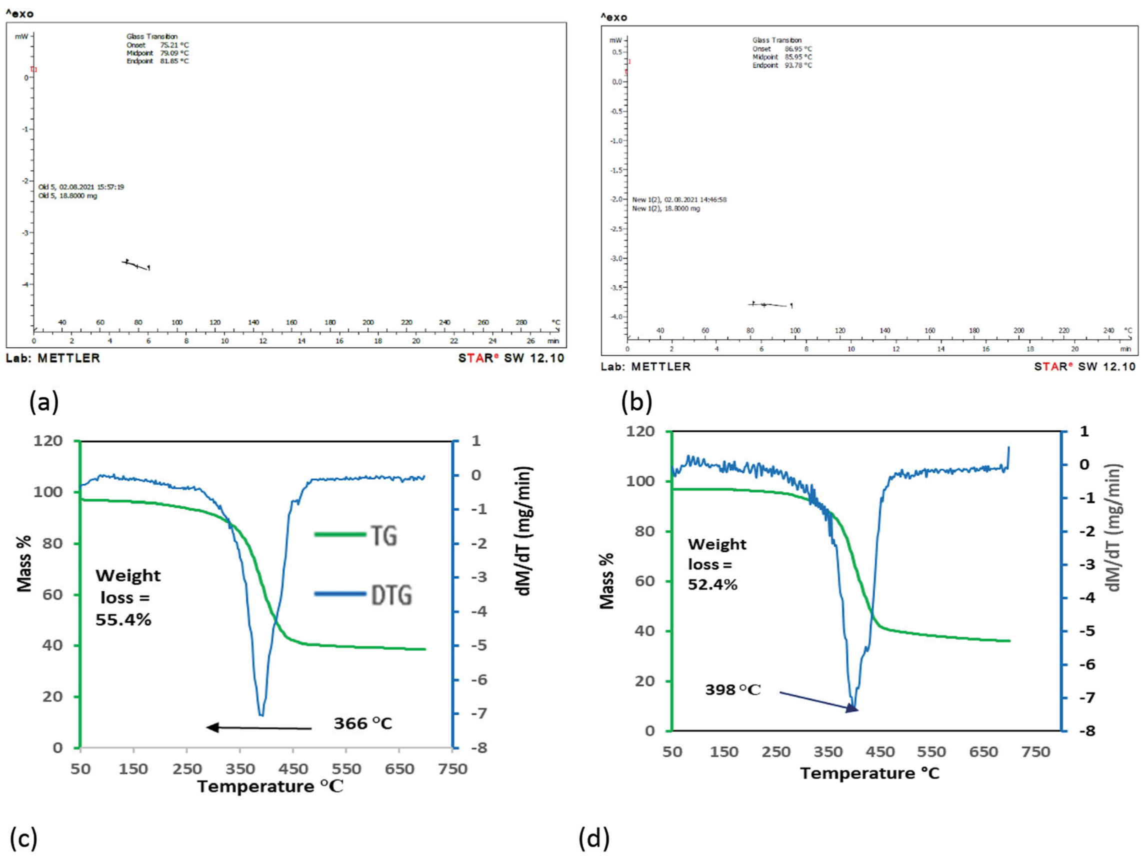


**Fig. 6** TG and DTG analysis (**a**) hydrotest failed sample (**b**) good pipe sample

the fibres. In case of hydrotest failed samples, volume fraction of fibres was observed to be very less compared to resin matrix; distribution of fibres was observed to be non-uniform (Fig. 3a). Numerous voids or porosities were observed in the sample compared to those of good FRP Pipe sample. Plenty of particle like features were observed in the matrix. Decohesion or separation between the matrix and particles were distinctly observed (Fig. 3a and b). Fibres were non-uniform and varying in size and large voids with entangled fibres inside observed for the hydrotest failed samples (Fig. 3c and d).

## EDX Analysis

Field emission gun scanning electron microscope (FEG-SEM) study of the samples was also carried out to identity different phases present in the samples. The analyses were performed at 15 keV accelerating voltage and 510–8 A probe current. The GRP pipes were coated with gold using a vacuum coater. The gold contribution was manually subtracted from the final EDX data. EDX analysis of particles shows significant content of Si and O suggesting presence of sand (50–90%) as shown in Table 1.

## Raman Spectroscopy Analysis

The Raman spectroscopy analysis were performed at 785 nm with a Renishaw, inVia Qontor system having a Nd-YAG laser source and equipped with a Centrus detector OFQM98 and grating 1200 l/mm. The continuous scan was checked for the spectral range from 98.87 to 3199.04 Raman shift/cm$^{-1}$. Raman spectroscopy is used to study resin and to identify the purity of the resin material. See Table 2.

In case of hydro test failed pipe sample terephthalic acid (TPA) and isophthalic acid (IPA) peaks along with orthophthalic acid (OPA) peaks were observed which indicates the resin material is not pure. Whereas in the good GRP pipe only, terephthalic acid (TPA) peaks were observed and the absence of isophthalic acid (IPA) and orthophthalic acid (OPA) peaks indicates high purity of resin sample in good GRP pipe [11, 12].

An terephthalic resin has a higher degree of crosslinking and increased chemical resistance than a standard orthophthalic polyester resin which makes isophthalic polyester resin more suitable for applications isophthalic resin is harder, has a higher flexural strength and shear strength than orthophthalic one (Figs. 4 and 5).

**Table 3** Values of glass transition temperature (Tg) for different samples

| Material | Onset *Tg* (°C) | Material | Onset *Tg* (°C) |
|---|---|---|---|
| Leaked (Sample #1) | 76.00 | Good (Sample #1) | 88.04 |
| Leaked (Sample #2) | 75.21 | Good (Sample #2) | 86.95 |
| Average (Leaked) | 75.60 | Average (New) | 87.49 |

## Temperature-modulated differential scanning calorimetry test (TMDSC)

TMDSC is a thermal analysis technique that has been found to be an accurate tool for measuring the temperatures of various transitions occurring in materials. In the present investigation, the TMDSC was employed to determine the glass transition temperature ($Tg$) value of the composite pipe materials. $Tg$ is the temperature range during which the polymer shifts from a tough glassy state to a soft rubbery state. The test was conducted from 30 to 250 °C at the heating rate of 10 °C/min. $Tg$ value of leaked pipe material showed a relatively lower value than that of new pipe material (Fig. 6a and b, Table 3). At temperatures above $Tg$, a polymer experiences a sudden drop in its mechanical stiffness. Typically, when mechanical stiffness is desired, a polymer's service temperature should be below its $Tg$.

Thermogravimetric ($TG$) curve indicates weight loss as a function of temperature. Derivative thermogravimetric (DTG) curve Indicates rate of weight loss as a function of temperature. Highest weight loss (55.4 %) was observed for hydrotest failed pipe sample, whereas good pipe sample

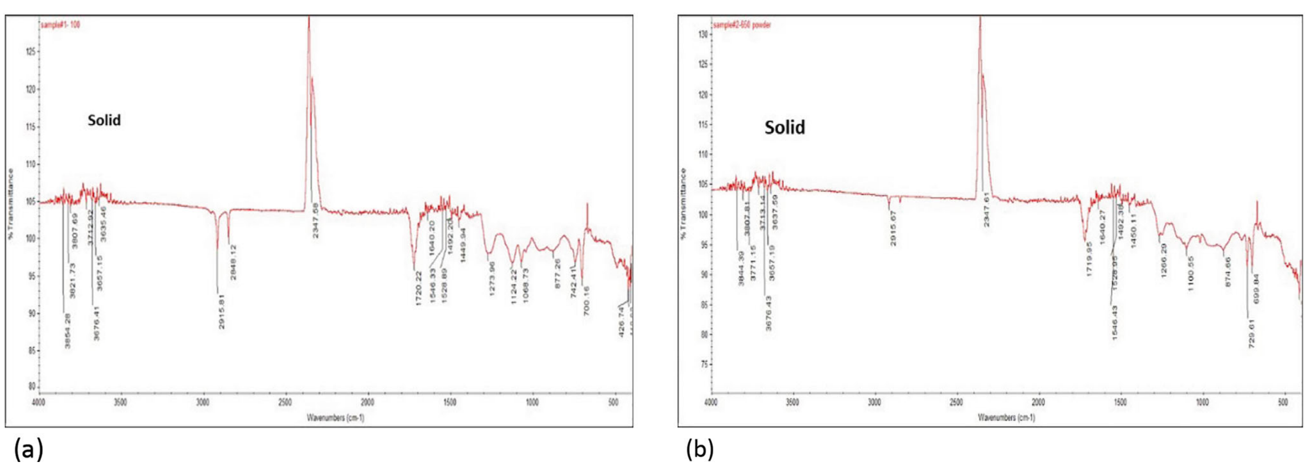


**Fig. 7** Fourier transform infrared spectrophotometers (FTIR) analysis (**a**) hydrotest failed pipe sample (**b**) good pipe sample

**Table 4** Peak assignments in FTIR analysis

| Description of peak | Peak position ($cm^{-1}$) | Good sample | Leaked sample | Reference |
|---|---|---|---|---|
| ν(C=O) carboxyl stretch | 1715 | √ | √ | Osterrothova and Jehlicka [12] |
| ν(C=C), C=C stretch | 1449 | √ | √ | |
| ν(C–O), carboxyl stretch | 1263 | √ | √ | |
| νas (C=O) & δ(COH) antisymetric stretch and in plane deformation in benzene ring | 1642 | √ | √ | Tellez et al. [15] |
| ν(CO) & δ(COH), strech and in plane deformation in benzene ring | 1117 | | √ | |
| γ(CCC) & δ(COH), out of plane and in plance deformation in benzene ring | 1017 | | | |
| δ(CCC), in plane vibration | 700 | √ | √ | Bardak et al. [13] |
| δ(CC), in plane deformation | 1073 | | √ | Bardak et al. [13] |

(52.4%) showed incrementally lower values. The decomposition temperature of hydrotest failed pipe sample at 366 °C was lower than good pipe sample (393 °C). This indicates that hydrotest failed pipe is relatively less thermally stable (Fig. 6c and d). With the increase in temperature, the ring stiffness, bending strength and damage displacement of GFRP pipes will show a decreasing trend for the hydrotest failed pipe sample. Both temperature and continuous fibre content have essential effects on the damage mode [13, 14].

### Fourier transform infrared spectrophotometers (FTIR) analysis

The FTIR analysis was done using a Nicolet Magna 550 Fourier transform infrared spectroscopy (FTIR) analyzer with a resolution of 4 $cm^{-1}$ in the range of 400–4000 $cm^{-1}$ wave number. FTIR analysis shows that the intensity of FTIR peaks for leaked or used pipe was lower than that of new or unused pipe. Peak assignments for both the samples are presented in Fig. 7a and b, and Table 4. From these observations, it is seen that peak position 1643 $cm^{-1}$ is present in case of the leaked pipe sample which is a characteristic assignment for TPA [15]. Thus, the leaked pipe sample is not pure in form which can also be correlated to observations of Raman analysis and is prone to failure.

## Conclusion

The GFRP composite pipes failed due to seepage during hydro test while laying out in the site due to inadequate manufacturing process, and usage of improper polymer/ resin material and non-uniform sand content along with non-prescribed fibre loading which might have initiated the failure of pipes during hydro test.

## References


1. M. Quanjin, R. Rejab, N.M., Kumar, Wireless technology applied in 3-axis filament winding machine control system using MIT app inventor, in IOP Conference Series: Materials Science and Engineering, (Vol. 469, p. 012030). IOP Publishing. (2019)
2. J.D. Diniz Melo, F. Levy Neto, G. de Araujo Barros, F.N. de Almeida Mesquita, Mechanical behavior of GRP pressure pipes with addition of quartz sand filler. J. Compos. Mater. **45**(6), 717–726 (2011)
3. J.D.D. Melo, G.A. Barros, Effect of quartz sand filler on mechanical properties of GRP pressure pipes. J. Adv. Mater. **41**(4), 28–39 (2009)
4. ASTM D 3517-96. Standard Specification for “GRP” (Glass-Fibre-Reinforced Thermosetting-Resin) Pressure Pipe. American Society for Testing and Materials.
5. ASTM D 3754-96. Standard Specification for “GRP” (Glass-Fibre-Reinforced Thermosetting-Resin) Sewer and Industrial Pressure Pipe. American Society for Testing and Materials.
6. ASTM D 3262-96. Standard Specification for “GRP” (Glass-Fibre-Reinforced Thermosetting-Resin) Sewer Pipe. American Society for Testing and Materials.
7. F. Adar, 2D COS of temperature-dependent Raman spectra of amorphous, non-oriented polyethylene terephthalate to separate molecular conformational changes from true crystallization. Spectroscopy. **33**, 12–20 (2018)
8. K. Krishnan, R.S. Krishnan, Raman and infrared spectra of ethylene glycol. Proc. Ind. Acad. Sci. A. **64**, 8 (1966)
9. ASME B31 Pressure Piping - Overview
10. ASTM D2412-21, Standard Test Method for Determination of External Loading Characteristics of Plastic Pipe by Parallel-Plate Loading
11. S. Dasa, G. Kumara, R. Chattia, S. Moniaa, S. Deya, A. Kumara, G. Mukhopadhyaya, Material Characterization of Buried GFRP Pipeline Failed during Hydrostatic Testing, Int. Res. J. Eng. Technol. **10**(9)

12. K. Osterrothova, J. Jehlicka, Raman spectroscopic identification of phthalic and mellitic acids in mineral matrices. Spectrochimica Acta Part A. **77**, 1092–1098 (2010)
13. F. Bardak, C. Karaca, S. Bilgili, A. Atac, T. Mavis, A.M. Asiri, M. Karabacak, E. Kose, Conformational, electronic, and spectroscopic characterization of isophthalic acid (monomer and dimer structures) experimentally and by DFT. Spectrochimica Acta Part A: Mol. Biomol. Spectrosc. **165**, 33–46 (2016)
14. R. Paseiro-Cerrato, S. MacMahon, C.D. Ridge, G.O. Noonan, T.H. Begley, Identification of unknown compounds from polyester cans coatings that may potentially migrate into food or food simulants. J. Chromatogr. A. **1444**, 106–113 (2016)
15. C.A. Tellez, E. Hollauer, M.A. Mondragon, V.M. Castano, Fourier transform infrared and Raman spectra, vibrational assignment, and ab initio calculations of terephthalic acid and related compounds. Spectrochimica Acta Part A. **57**, 993–1007 (2001)